HEP'99 # 5_563
Submitted to Pa 5
Pl 5

DELPHI 99-132 CONF 319
15 June 1999

A Study of Charged Kaon Production in One-Prong Tau Decays

Preliminary

DELPHI Collaboration

Paper submitted to the HEP'99 Conference
Tampere, Finland, July 15-21

A Study of Charged Kaon Production in One-Prong Tau Decays

Preliminary

DELPHI Collaboration

J.M.López[1], F.Matorras[1], K.Pachjel[2], B.Stugu[2]

Abstract

Using LEP-1 data collected in the DELPHI detector, we have measured the τ decay branching ratios for modes containing one charged kaon, $\tau^- \to K^-\nu_\tau$, $\tau^- \to K^- \geq 1\pi^0\nu_\tau$, $\tau^- \to K^-K^0_L\nu_\tau$ and $\tau^- \to K^-K^0_L \geq 1\pi^0\nu_\tau$, as well as for the inclusive decay $\tau^- \to K^- \geq 0K^0 \geq 0\pi^0\nu_\tau$. To optimise the charged kaon identification a combination of information from the DELPHI Ring-imaging Cherenkov detector and the TPC ionisation is used, allowing K/π separation over the full momentum range.

[1]Universidad de Cantabria, Santander
[2]University of Bergen

1 Introduction

In this paper we update the measurement of the tau decay branching ratios to $\tau^- \to K^-\nu_\tau$, $\tau^- \to K^- \geq 1\pi^0\nu_\tau$ and $\tau^- \to K^- \geq 0K^0 \geq 0\pi^0\nu_\tau$ published in [1] and those presented in previous conferences [2] and we include new results for the channels $\tau^- \to K^-K^0_L\nu_\tau$ and $\tau^- \to K^-K^0_L \geq 1\pi^0\nu_\tau$. Data taken by the DELPHI detector around the Z peak from 1993 to 1995 was added.

Measurement of these branching ratios requires the rejection of $\tau^- \to \pi^-\nu_\tau$ and $\tau^- \to \pi^- \geq 1\pi^\circ\nu_\tau$ decays. These decay modes have branching ratios more than an order of magnitude larger, between ≈ 20 and ≈ 60 depending on the number of accompanying π^0's [3]. As the only difference in these channels is the existence of a charged π or K, charged pion rejection of order 100 is needed. Another important issue is to maintain this rejection with significant efficiency over the whole momentum spectra. This is especially difficult for the $\tau^- \to K^-\nu_\tau$ decay mode whose momentum spectrum is almost flat up to the maximum energy of 45.6 GeV. To achieve this goal the particle identification of two DELPHI subdetectors have been combined: the ionisation deposition in the TPC, $\frac{dE}{dx}$, and the Ring Imaging Cherenkov. The DELPHI detector is described in [4].

2 Event sample

The data sample corresponds to the data taken by DELPHI during 1993 (15.7 pb^{-1} at $E_{cm} = 91.2$ GeV, 9.4 pb^{-1} at $E_{cm} = 89.2$ GeV and 4.5 pb^{-1} at $E_{cm} = 93.2$ GeV), 1994 (47.4 pb^{-1} at $E_{cm} = 91.2$ GeV) and 1995 (14.3 pb^{-1} at $E_{cm} = 91.2$ GeV, 9.2 pb^{-1} at $E_{cm} = 89.2$ GeV and 9.3 pb^{-1} at $E_{cm} = 93.2$ GeV).

Selected according to the criteria described in [5], the event sample consisted of a high purity sample of dileptonic events ($e^+e^- \to e^+e^-$, $\mu^+\mu^-$, $\tau^+\tau^-$) where cosmic rays, $e^+e^- \to q\bar{q}$ and $e^+e^- \to (e^+e^-)X$ two-photon events had been removed.

This selection was used to produce a sample of dileptonic decays of the Z with 87% efficiency for $\tau^+\tau^-$ events within the polar angle fiducial region, calculated from simulated data. The cosmic ray contamination was negligible.

The final sample corresponded to 80000 $\tau^+\tau^-$ pairs.

In all analyses, samples of simulated events were used which had been passed through a detailed simulation of the detector response [6] and reconstructed with the same program as the real data. The Monte Carlo event generators used were: KORALZ [7] for $e^+e^- \to \tau^+\tau^-$ events; DYMU3 [8] for $e^+e^- \to \mu^+\mu^-$ events; BABAMC [9] for $e^+e^- \to e^+e^-$ events; JETSET 7.3 [10] for $e^+e^- \to q\bar{q}$ events; Berends-Daverveldt-Kleiss [11] for $e^+e^- \to e^+e^-e^+e^-$ events, $e^+e^- \to e^+e^-\mu^+\mu^-$ and $e^+e^- \to e^+e^-\tau^+\tau^-$ events.

3 Particle identification

3.1 Charged kaon and pion separation

The DELPHI pion and kaon separation is based on two subdetectors, the ionisation as measured in the TPC and the Cherenkov signals in the Liquid and Gas RICH. The Liquid RICH does not provide any additional information in this case, because the signals are already saturated at the minimum kinematically allowed laboratory momentum of

≈3.5 GeV/c of the kaons produced in decays of τ particles with laboratory momentum 45 GeV/c.

To use $\frac{dE}{dx}$ information, we built several "pull" variables called, $\Pi_{dE/dx}$, defined as the difference of the measured value of the ionisation deposition in the TPC and the predicted value for a given particle type, divided by the expected uncertainty.

$$\Pi_{dE/dx} = \frac{(dE/dx)_{meas} - (dE/dx)_{expec}}{\sigma(dE/dx)} \tag{1}$$

We thus define $\Pi^{\pi}_{dE/dx}$ for the expected response for a pion, $\Pi^{K}_{dE/dx}$ for that of a kaon, etc. By construction, this variable follows a Gaussian distribution with mean zero and unit standard deviation, when the particle type used in the expectation corresponds to that of the measured particle (called the "right hypothesis"), and it is displaced when it does not (the "wrong hypothesis"). Both pion and kaon hypotheses were used. To ensure a good measurement of the ionisation, only tracks with a signal in at least 100 TPC wires out of a maximum 192 were retained.

The RICH response was different according to the particle momentum. For particles with momentum less than 8.5 GeV/c, kaons are below the Cherenkov threshold, while pions give a signal. This is the veto region, where kaons are identified because they do not emit Cherenkov radiation. In Fig. 1 the distribution is shown of the number of observed photoelectrons (electrons generated by photoionization induced by Cherenkov photons) for both particles in this momentum range. For momenta above 8.5 GeV/c both pions and kaons radiate and a Cherenkov ring is reconstructed when at least two photoelectrons are detected. In a manner equivalent to that used for the TPC ionisation deposition, a set of pull variables Π_{RICH} were constructed, with the measured and expected ring opening angle. A tight track selection was required to guarantee a good RICH response: the extrapolation of the track to the RICH had to lie in an active part of the subdetector and within its acceptance, and for ring identification, to have at least two photoelectrons and no noise around the track.

If the track fulfils both TPC ionisation and RICH quality requirements, the K/π identification of both subdetectors can be combined into a single variable. For a given momentum, the distribution of $\Pi_{dE/dx}$ versus Π_{RICH} is a 2-dimensional Gaussian, with zero correlation, unit variance in both axes and centred at the origin for the "right hypothesis" or centred at $(\mu_{dE/dx}(p), \mu_{RICH}(p))$ for the "wrong hypothesis". These μ_x are the separation between π and K hypothesis as shown in Fig. 1. The optimal way to combine both pull variables is a momentum dependent rotation in the $\Pi_{dE/dx} - \Pi_{RICH}$ plane:

$$\Pi_{comb} = \sin\alpha \cdot \Pi_{dE/dx} + \cos\alpha \cdot \Pi_{RICH} \tag{2}$$

$$\tan\alpha = \frac{\mu_{dE/dx}(p)}{\mu_{RICH}(p))} \tag{3}$$

In Fig. 1 we show the separation between kaons and pions in number of standard deviations, for the three cases. The combination of both subdetectors provides almost 2σ or better over the full momentum spectrum.

A second procedure consisted in using the RICH Cherenkov angle to estimate the mass of the particle. While the separation between the pull variables for different particle hypotheses is a function of the particle momentum, mass differences stay constant.

Instead, the mass resolution changes with momentum. The relevant quantity to use is the square of the mass, m^2, as fast particles often will give measured Cherenkov angles corresponding to velocities above (but compatible with) $\beta = 1$. This corresponds to a negative value for the m^2 estimate. Fig. 2 shows the distribution of the reconstructed m^2 in three different momentum ranges.

3.2 Neutral kaons and pions

K_L^0 identification was performed on the basis of the energy deposition on the Hadron Calorimeter (HCAL). In most cases the HCAL granularity was not enough to separate the neutral energy deposition from that of the accompanying charged hadron. To allow an efficient rejection and identification all the energy deposited in a cone of 10° around the track was taken into account. An event was considered as including a K_L^0 when this energy divided by the momentum of the charged hadron was larger than 1.5.

The K_S^0 were in general rejected if they decayed to $\pi^+\pi^-$ using the track multiplicity, but were irreducible background to the $\tau^- \to K^- \geq 1\pi^0\nu_\tau$ when decaying to $\pi^0\pi^0$. However, this background was subtracted according to world averages [3] and taking into account the differences in the selection efficiencies produced by the different kinematics (mainly the momentum spectra of the kaons).

A simple π^0 identification algorithm was used demanding only the existence of at least one identified photon or π^0. Since no attempt is made to count π^0's in the final state, this requirement was found to give good separation while retaining a high efficiency.

A photon was defined as either a shower in the electromagnetic calorimeter not associated to a track extrapolation and fulfilling quality cuts based on minimum energy and shower profile or a converted photon reconstructed from an electron-positron pair observed in the tracking subdetectors [12]. The π^0 identification is described in more detail in [12].

3.3 Electron and muon rejection

Although most leptonic τ decays could be rejected with the kaon and pion identification variables explained above, some loose cuts, nearly 100% efficient for kaons were applied to further reduce this background. It was required that the track had no associated hits in the muon chambers and that the associated energy on the electromagnetic calorimeter was less than 70% of the measured momentum of the track. More details on the electron and muon rejection can be found in [12, 13].

4 Track selection and detector quality

Due to kinematical constraints of the τ decays, kaons are produced with at least 3.5 GeV/c momentum. Therefore only τ decays with a single track of momentum greater than 3.5 GeV/c where retained. In addition to the previously described requirements on the track to use the RICH in the identification it was requested for the veto region, below 8.5 GeV, that the track have an associated hit in the Outer Detector, the charged track reconstruction detector placed on the radial exterior of the RICH. This ensured a correct extrapolation and reduced the background from pions with no photoelectrons associated due to an incorrect extrapolation of the track in the RICH.

5 Measurement of the branching ratios

The selection was applied in three steps, first to the whole one-prong hadronic sample, giving an inclusive measurement, BR($\tau^- \to K^- \geq 0K^0 \geq 0\pi^0\nu_\tau$). Here, both K^0_S and K^0_L long are included. Then, the sample was divided in four according to the number of identified π^0's and K^0_L and the branching ratios for the decays $\tau^- \to K^-\nu_\tau$, $\tau^- \to K^- \geq 1\pi^0\nu_\tau$, $\tau^- \to K^-K^0_L\nu_\tau$ and $\tau^- \to K^-K^0_L \geq 1\pi^0\nu_\tau$ were measured. Finally, only $\tau^- \to K^-\nu_\tau$ and $\tau^- \to \pi^-(K^-)\nu_\tau$ were measured, fixing the other two branching ratios to the world averages to increase the statistical precision.

Several cases were considered depending on the track quality cuts and momentum. The cuts were defined in terms of n, the difference between the kaon and pion hypothesis in number of standard deviations, to allow adjustment according to the requirement of the selection (i.e. to improve efficiency at the expense of purity or vice-versa)

1. if both the RICH and TPC track requirements were fulfilled and the momentum was greater than 8.5 GeV/c, a cut on the combined pull variable was performed: $\Pi^\pi_{comb} < -n$.

2. if both the RICH and TPC track requirements were fulfilled and the momentum was less than 8.5 GeV/c, it was required that there be no photoelectrons in the RICH and that $\Pi^\pi_{dE/dx} < 2 - n$.

3. if the track failed the RICH track requirement, a cut at $\Pi_{dE/dx} < -n$ was performed.

4. if the track failed the TPC track requirement and the momentum was less than 8.5 GeV/c the event was accepted if there were no photoelectrons in the RICH

5. if the track failed the TPC track requirement and the momentum was more than 8.5 GeV/c the event was accepted when $\Pi^\pi_{RICH} < -n$.

6. if the track failed both the RICH and TPC track requirements, the event was rejected.

In the case 2 above, as the cut on the photoelectron number already gave good separation the cut on $\Pi_{dE/dx}$ was loosened by 2σ. In all cases, it was also required that the track was compatible with the kaon hypothesis, $|\Pi^K| < 3$. The value of n=2.25 was chosen as the one giving the better statistical precision, although purer samples could be obtained with a reasonable efficiency tightening the cut.

The alternative analysis using m^2 selected the candidates according to the following criteria. Kaon candidates were selected by requiring $m^2 > 0.18\,(\mathrm{GeV}/c^2)^2$. For low momenta (below about 15 GeV) this selects a clean sample of kaons, but the pion contamination increases with momentum. The pion background can be substantially reduced by imposing requirements on the ionization energy in the TPC. Requiring that the dE/dx pull variable for the pion hypothesis should be smaller than -0.5 eliminates about 65 % of the remaining pion background, with virtually no loss of kaons.

For momenta below the Cherenkov threshold, kaons were selected by requiring that no ring should be found in the RICH. This gives a very clean sample of kaons.

Finally, for tracks where the reconstruction quality did not permit proper use of the RICH information, and for events where the RICH information was not available, kaons

were selected by requiring that the pull variable for the pion hypothesis should be less than -2.0.

Both approaches gave similar efficiencies and purities and compatible results for the branching ratios.

In Fig. 3 the efficiencies and misidentification probabilities are shown as a function of the momentum for different cuts.

A total number of 1265 $\tau^- \to K^- \geq 0K^0 \geq 0\pi^0\nu_\tau$ candidates were found, with an average efficiency of 45% and a background of 32% from other τ decays and other non-τ processes. For the exclusive measurements, the events were classified as $\tau^- \to K^-\nu_\tau$, $\tau^- \to K^- \geq 1\pi^0\nu_\tau$, $\tau^- \to K^-K^0_L\nu_\tau$ or $\tau^- \to K^-K^0_L \geq 1\pi^0\nu_\tau$ according to the existence of a π^0 or K^0_L. The efficiency matrix and backgrounds from other channels are summarised in Table 1. With these cuts a sample of 493 $\tau^- \to K^-\nu_\tau$, 640 $\tau^- \to K^- \geq 1\pi^0\nu_\tau$, 59 $\tau^- \to K^-K^0_L\nu_\tau$ and 73 $\tau^- \to K^-K^0_L \geq 1\pi^0\nu_\tau$ events were selected. All four branching ratios were obtained simultaneously from the inversion of the efficiency matrix. The results were:

$$BR(\tau^- \to K^- \geq 0K^0 \geq 0\pi^0\nu_\tau) = (1.607 \pm 0.066)\%.$$
$$BR(\tau^- \to K^-\nu_\tau) = (0.633 \pm 0.051)\%;$$
$$BR(\tau^- \to K^- \geq 1\pi^0\nu_\tau) = (0.559 \pm 0.069)\%;$$
$$BR(\tau^- \to K^-K^0_L\nu_\tau) = (0.093 \pm 0.036)\%;$$
$$BR(\tau^- \to K^-K^0_L \geq 1\pi^0\nu_\tau) = (0.115 \pm 0.048)\%;$$

or alternatively, fixing the branching ratios of the channels with K^0_L to the world averages [3]:

$$BR(\tau^- \to K^-\nu_\tau) = (0.648 \pm 0.045)\%;$$
$$BR(\tau^- \to K^- \geq 1\pi^0\nu_\tau) = (0.589 \pm 0.057)\%;$$

The errors are statistical only. In the inclusive channel, $\tau^- \to K^- \geq 0K^0 \geq 0\pi^0\nu_\tau$, both K^0_S and K^0_L components are included, independently of the K^0 decay. Tightening and loosening the cuts by $\frac{1}{2}\sigma$ showed good stability in the results.

	Efficiency				Background
	$K^-\nu_\tau$	$K^- \geq 1\pi^0\nu_\tau$	$K^-K^0_L\nu_\tau$	$K^-K^0_L \geq 1\pi^0\nu_\tau$	
$K^-\nu_\tau$	0.42	0.05	0.19	0.05	0.22
$K^- \geq 1\pi^0\nu_\tau$	0.03	0.38	0.10	0.24	0.50
$K^-K^0_L\nu_\tau$	0.02	0.01	0.19	0.02	0.20
$K^-K^0_L \geq 1\pi^0\nu_\tau$	0.00	0.02	0.04	0.17	0.37
$K^- \geq 0K^0 \geq 0\pi^0\nu_\tau$	0.47	0.46	0.52	0.48	0.32

Table 1: Selection efficiency for the exclusive decays and background from other channels. The rows represent the selected channels, while the first four columns represent the generated decays. The numbers are the probability that a given original decay were classified in a given class. The last column represent the background from other tau decays and non tau decays in each class.

6 Cross checks and systematic errors

All variables were cross checked with different test samples, comparing data and simulation. These test samples were selected independently of the RICH and the TPC ionisation information. Three different samples were used:

- electrons selected with the information of the electromagnetic calorimeter
- muons selected with the hadron calorimeter and muon chambers
- single prong pions and kaons selected with all the above subdetectors

All these samples had at most 2% background from other decays. Due to the difficulty of separating pions and kaons, and the small fraction of kaons, no high momentum kaon test sample in an isolated environment could be selected without strong biases in the momentum and with low number of events. However, checks were carried out with the $\pi+K$ sample, enhancing the K component or removing it with cuts on the RICH variables to check the ionisation and on $\Pi_{dE/dx}$ to check the RICH. The kaon enriched samples had a fraction of K from 30 to 50 %, depending on the momentum range. The pion sample had a $2-3\%$ fraction of kaons. Plots for these variables are shown in Figs. 4 and 5. In all cases the agreement of data and MonteCarlo was good. However, to give a conservative upper estimate the data and simulated data distributions were fitted to Gaussians and the statistical error on the difference between the means and variances was propagated to the measured branching ratios as a systematic uncertainty. These uncertainty are listed in Table 2. Equivalently, the statistical error on the difference on the fraction of tracks with no associated photoelectron was taken. This had two effects; for the low momentum particles in the RICH veto region it implied a larger pion background fulfilling the veto requirement, while for higher momentum particles it meant larger fraction of tracks measured with $\Pi_{dE/dx}$ only. Both these effects were found to give a negligible contribution to the systematic uncertainties. The γ and π^0 reconstruction efficiency was checked in a similar way as in [12] and its propagation to the branching ratios is also listed on table 2. The track reconstruction and selection was also checked with the test samples and the statistical error of the difference between data and MonteCarlo efficiency was propagated as a systematic effect. It had a negligible contribution to the error. The requirements on the extrapolation to the RICH were studied in a similar way.

7 Summary and conclusions

The one-prong decays of the τ containing charged kaons have been analysed on 1993 to 1995 DELPHI data around the Z^0 peak. The combination of the TPC ionisation information together with that provided by the Ring Imaging Cherenkov allowed a good pion/kaon separation over all the momentum spectra, from 3.5 GeV/c to 45.5 GeV/c. The results were:

$$\begin{aligned}
BR(\tau^- \to K^- \geq 0K^0 \geq 0\pi^0\nu_\tau) &= (1.607 \pm 0.066_{stat} \pm 0.057_{sys})\%; \\
BR(\tau^- \to K^-\nu_\tau) &= (0.648 \pm 0.045_{stat} \pm 0.043_{sys})\%; \\
BR(\tau^- \to K^- \geq 1\pi^0\nu_\tau) &= (0.589 \pm 0.057_{stat} \pm 0.043_{sys})\%; \\
BR(\tau^- \to K^-K^0_L\nu_\tau) &= (0.093 \pm 0.036_{stat} \pm 0.024_{sys})\%; \\
BR(\tau^- \to K^-K^0_L \geq 1\pi^0\nu_\tau) &= (0.115 \pm 0.048_{stat} \pm 0.028_{sys})\%,
\end{aligned}$$

error source	$K^-\nu_\tau$	$K^- \geq 1\pi^0\nu_\tau$	$K^-K^0_L\nu_\tau$	$K^-K^0_L \geq 1\pi^0\nu_\tau$	$K^- \geq 0K^0 \geq 0\pi^0\nu_\tau$
dE/dx calibration	0.020	0.020	0.010	0.010	0.030
Ring calibration	0.020	0.020	0.010	0.010	0.030
Photoelectrons	–	–	–	–	–
γ identification	0.006	0.006	–	–	–
K^0_L identification	0.020	0.020	0.015	0.015	–
Branching Ratios	0.006	0.012	–	–	0.028
Track selection	–	–	–	–	–
Rich status	0.010	0.010	0.002	0.002	0.015
MC statistics	0.015	0.020	0.012	0.019	0.022
Total	0.043	0.043	0.024	0.028	0.057

Table 2: Systematic errors in % for the fit method.

The first three branching ratios were already been measured by DELPHI with 1992 data in [1] (the quoted error is the total error):

$$BR(\tau^- \to K^- \geq 0K^0 \geq 0\pi^0\nu_\tau) = (1.54 \pm 0.24)\%;$$
$$BR(\tau^- \to K^-\nu_\tau) = (0.85 \pm 0.18)\%;$$
$$BR(\tau^- \to K^- \geq 1\pi^0\nu_\tau) = (0.69 \pm 0.25)\%,$$

the results are in agreement, and can thus be combined:

$$BR(\tau^- \to K^- \geq 0K^0 \geq 0\pi^0\nu_\tau) = (1.599 \pm 0.064_{stat} \pm 0.052_{sys})\%;$$
$$BR(\tau^- \to K^-\nu_\tau) = (0.670 \pm 0.044_{stat} \pm 0.040_{sys})\%;$$
$$BR(\tau^- \to K^- \geq 1\pi^0\nu_\tau) = (0.597 \pm 0.056_{stat} \pm 0.040_{sys})\%;$$

These results are in agreement with the world averages [3].

References

[1] DELPHI collaboration, Phys. Lett. B334 (1994) 435.

[2] DELPHI collaboration, A Study of Charged Kaon Production in One-Prong Tau Decays, ICHEP'98 (Pa 6 Pl 8 #247), Vancouver Canada

[3] Review of Particle Physics, Europ. Phys. Jour. C3, 1 (1998).

[4] DELPHI Collaboration, Nucl. Instr. and Meth. **A303** (1991) 233.
DELPHI Collaboration, Nucl. Inst. and Meth. **A378** (1996) 57.

[5] DELPHI collaboration, Zeit. Phys. C67 (1995) 183.

[6] "DELSIM Reference Manual", DELPHI Note 89-68, Sept. 1989, (unpublished).

[7] S.Jadach and Z.Was, Comp. Phys. Com. **36** (1985) 191;
S.Jadach, B.F.L.Ward and Z.Was, Comp. Phys. Com. **66** (1991) 276.

[8] J. E. Campagne and R. Zitoun, Z. Phys. **C43** (1989) 469.

[9] F. A. Berends, W. Hollik and R. Kleiss, Nucl. Phys. **B304** (1988) 712.

[10] T.Sjöstrand, Comp. Phys. Comm. **27** (1982) 243, ibid. **28** (1983) 229;
T.Sjöstrand and M. Bengtsson, Comp. Phys. Comm. **43** (1987) 367;
T.Sjöstrand, "PYTHIA 5.6 JETSET 7.3 Physics and manual", report CERN-TH 6488/92 (1992).

[11] F.A.Berends, P.H.Daverveldt, R.Kleiss, Phys. Lett. **B148** (1984) 489;
Comp. Phys. Comm. **40** (1986) 271.

[12] DELPHI collaboration, Measurement of τ hadronic branching fractions, this conference (Pa 5 Pl 5 HEP99 #5_511)

[13] DELPHI collaboration, Measurement of τ leptonic branching fractions, this conference (Pa 5 Pl 5 HEP99 #5_107), also CERN/EP 99–46

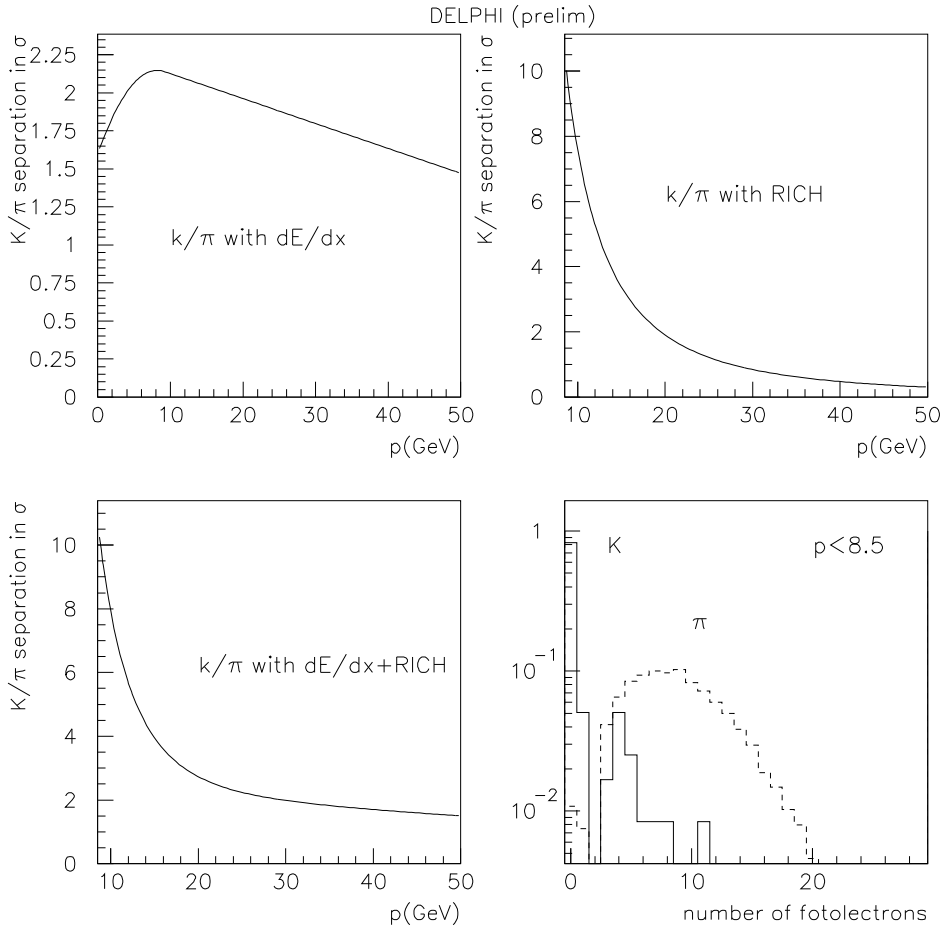

Figure 1: Kaon/pion separation for the different π/K identification variables. Top left: $\Pi_{dE/dx}$ only. Top right: Π_{RICH} only. Bottom left: the combined RICH+dE/dx variable Π_{comb}. Bottom right: the number of photoelectrons in the veto region for simulated pions (solid line) and kaons (dashed line).

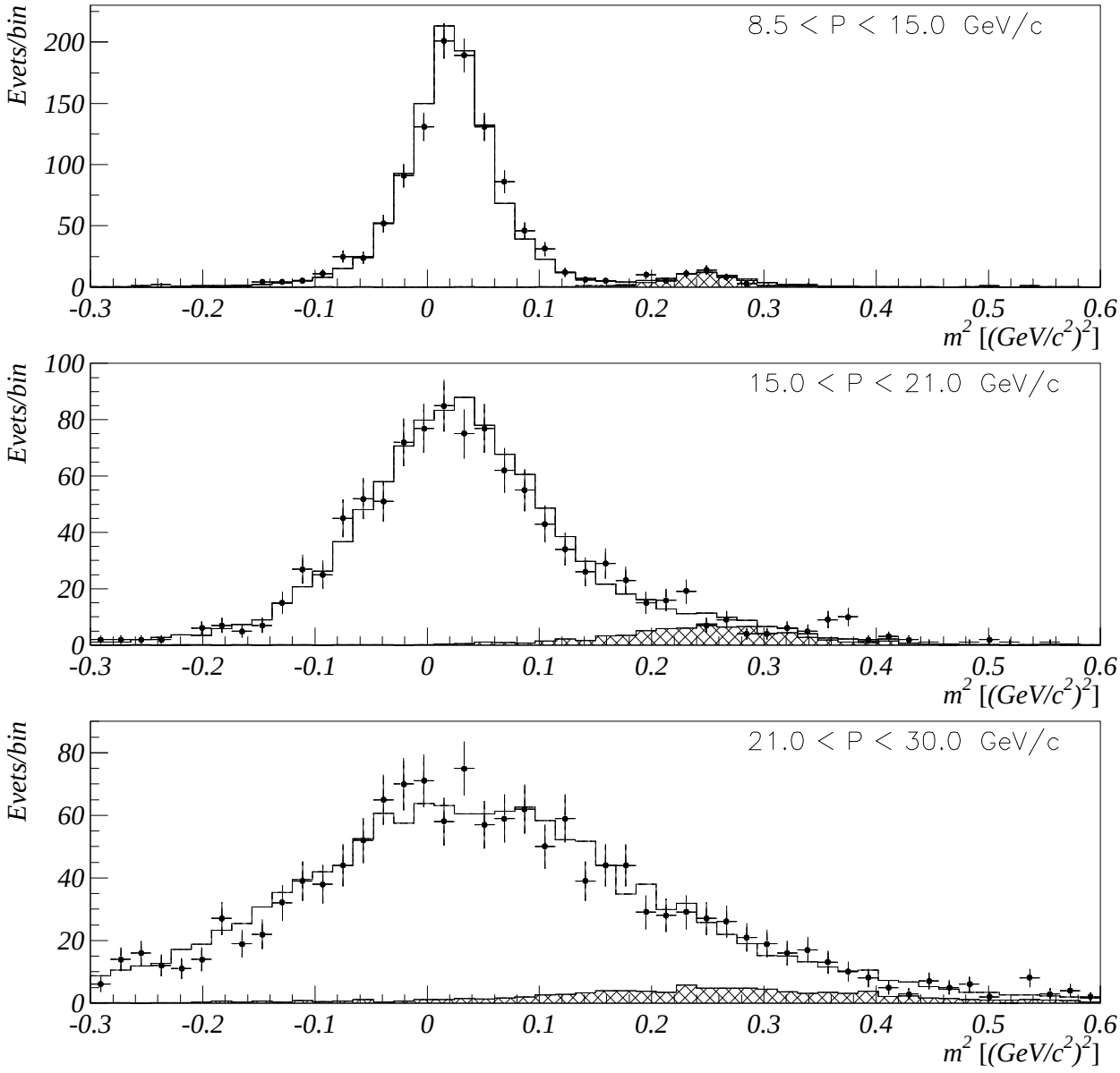

Figure 2: Distributions of the reconstructed m^2 in three different momentum ranges. The points represent the data, the open histogram represents The Monte Carlo simulation while the hatched histogram represents the simulated kaons. The plots contain data from the years 1993, 1994 and 1995.

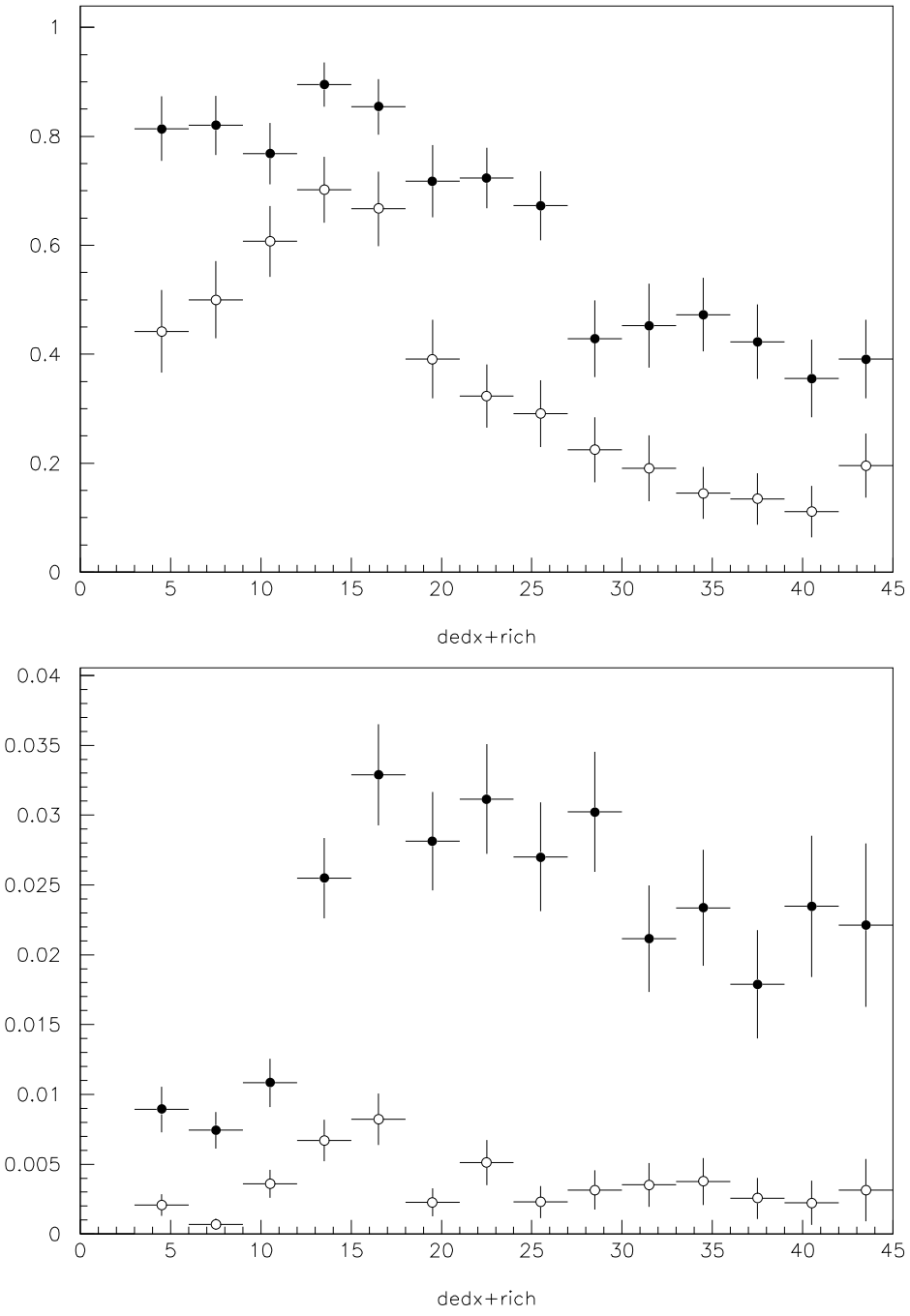

Figure 3: Top plot: kaon identification efficiency, calculated using simulated data, as a function of momentum for tight cut (open circles) and loose cut (solid dots). Bottom plot: $\pi \rightarrow K$ misidentification probability, calculated using simulated data, as a function of momentum for tight cut (open circles) and loose cut (solid dots). In both plots, the horizontal axis is momentum in units of GeV/c and the vertical axis is the efficiency/probability.

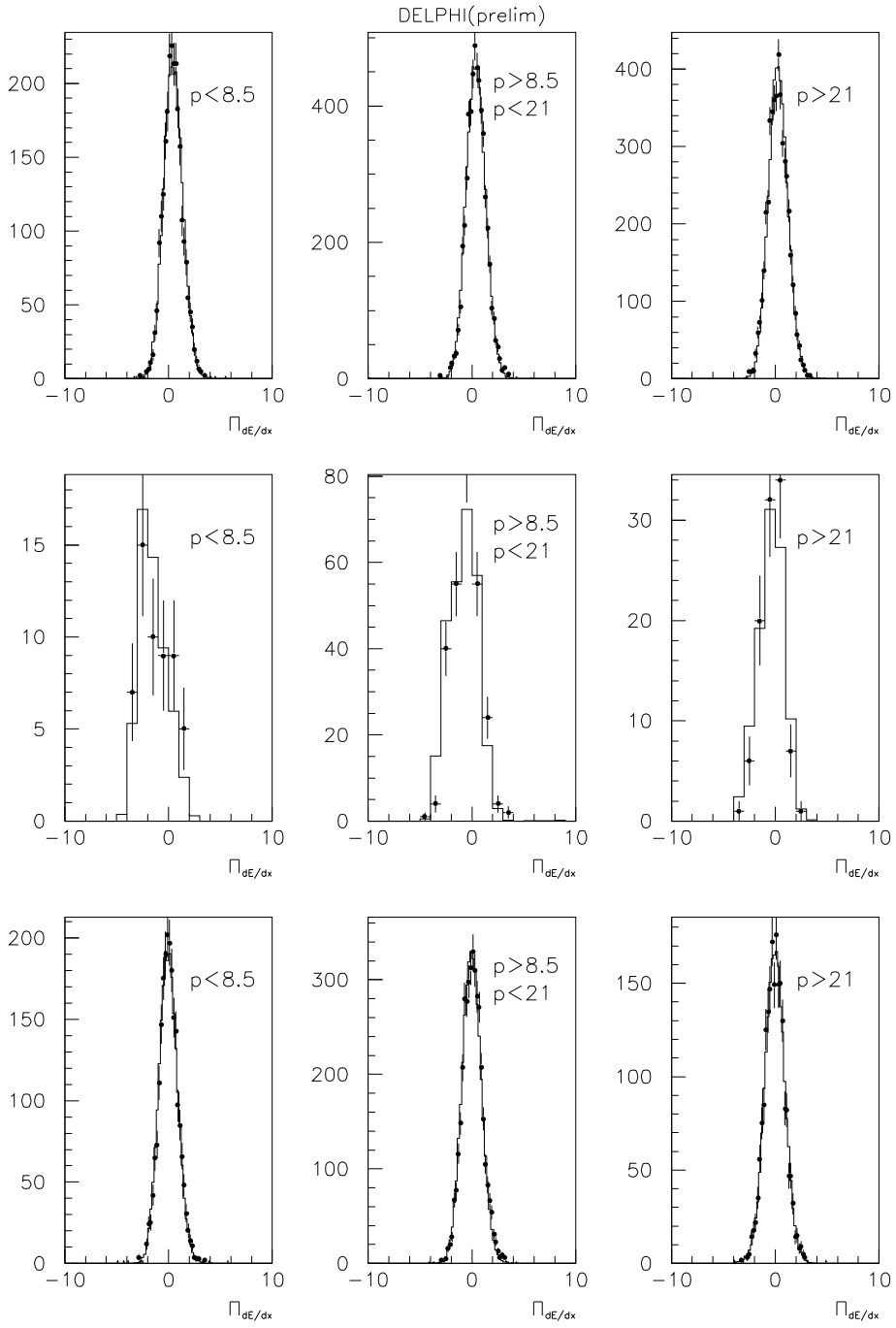

Figure 4: Data-simulation comparison for $\Pi_{dE/dx}$ for pion hypothesis in different momentum ranges for different test samples. Top figures correspond to muon test samples, centre plots to the kaon enriched sample and the bottom plots to the pion test sample. Dots are data, the solid line is simulation.

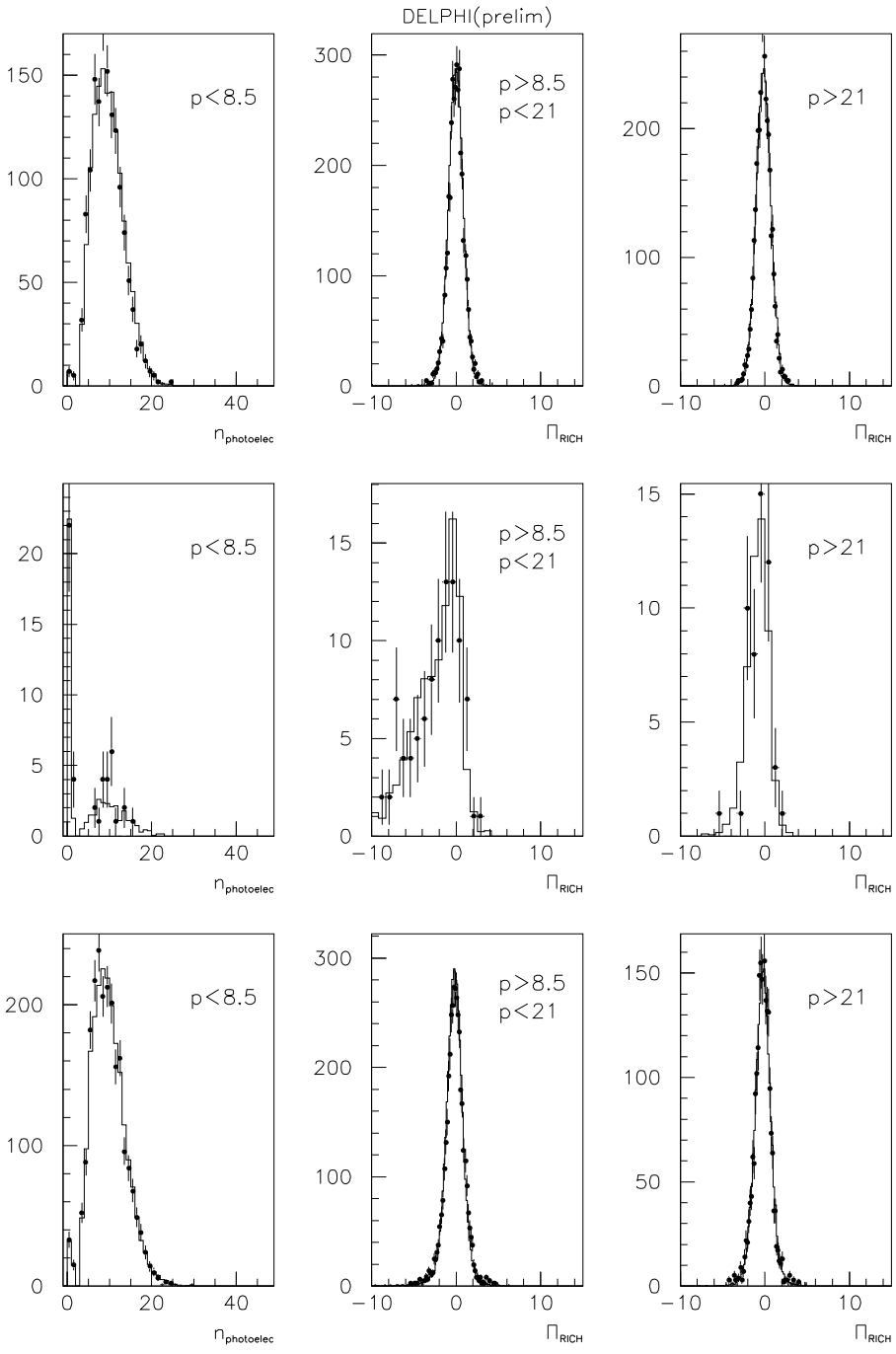

Figure 5: Data-simulation comparison for the RICH variables for different test samples. Left hand plots correspond to the number of photoelectrons in the veto region, centre and right hand plots correspond to Π_{RICH} for pion hypothesis in different momentum ranges. Top figures correspond to muon test samples, centre plots to the kaon enriched sample and the bottom plots to the pion test sample. Dots are data, the solid line is simulation.